Role of Phospholipid Scramblase 3 in the Regulation of Tumor Necrosis Factor-α-Induced Apoptosis[†]

Jihua Liu,[‡] Raquel F. Epand,[§] David Durrant,[||] Douglas Grossman,[⊥] Nai-wen Chi,[||] Richard M. Epand,*[,§] and Ray M. Lee*[,‡,#]

Department of Pharmaceutics and Pharmaceutical Chemistry and Huntsman Cancer Institute, University of Utah, Salt Lake City, Utah 84112, Department of Biochemistry and Biomedical Sciences, McMaster University, Hamilton, ON L8N 3Z5, Canada, Department of Internal Medicine, University of California, San Diego, La Jolla, California 92093, and Massey Cancer Center, Virginia Commonwealth University, Richmond, Virginia 23298

Received September 29, 2007; Revised Manuscript Received January 25, 2008

ABSTRACT: In tumor necrosis factor-α (TNF-α)-induced apoptosis, tBid is targeted to mitochondria and causes cytochrome *c* release. We investigated the regulation of tBid-induced cytochrome *c* release and apoptosis by phospholipid scramblase 3 (PLS3). Overexpression of PLS3 enhanced, whereas downregulation of PLS3 delayed, TNF-α-induced apoptosis and targeting of tBid to mitochondria. On the basis of the theory that tBid targets mitochondrial cardiolipin, we hypothesize that PLS3 enhances translocation of cardiolipin to the mitochondrial surface to facilitate tBid targeting. NAO, a cardiolipin binding dye, was first used to quantify the distribution of cardiolipin. Overexpression of PLS3 increases, whereas downregulation of PLS3 decreases, the percentage of cardiolipin on the mitochondrial surface. Determination of the tBid binding capacity on the mitochondrial surface by FITC-labeled tBid(G94E) also confirmed that tBid binding capacity increased upon PLS3 overexpression and decreased with downregulation of PLS3. PLS3 activity, determined by a lipid flip-flop assay, was activated by calcium and tBid but inhibited by Bcl-2. Mutation of the calcium binding motif abolishes the lipid flip-flop activity of PLS3. PLS3 and tBid may form a bidirectional positive feedback loop that is antagonized by Bcl-2. Overexpression of PLS3 does not affect mitochondrial potential but does interfere with mitochondrial respiration and production of reactive oxygen species. These studies thus establish PLS3 as an important downstream effector of Bcl-2 and tBid in apoptosis.

Regulation of apoptosis is central to development and neoplastic transformation. There are two major pathways in apoptosis signaling, the intrinsic and extrinsic pathways. The intrinsic pathway is activated by DNA damage, triggering mitochondrial cytochrome *c* release and activation of Apaf-1 and caspase 9 (*1*). The extrinsic pathway is activated by TNF-α[1] death receptors, which activate caspase 8 and downstream caspases. Bid, a BH3-only Bcl-2 family member, is cleaved by caspase 8, and the carboxyl terminus (tBid) translocates to mitochondria to promote apoptotic events (*2*). These pathways have physiological significance, as shown in Bid-deficient mice which display resistance to Fas-induced hepatocellular apoptosis (*3*). Cardiolipin (CL) was proposed as the mitochondrial target of tBid (*4*) and subsequently demonstrated to be essential for tBid to form a supramolecular complex with Bax (*5*). Preincubation of mitochondria with the CL-binding dye NAO inhibited mitochondrial targeting of tBid (*6*), supporting the notion that CL is the specific target of tBid. The same study also confirmed that tBid preferentially localizes to the mitochondrial contact zone, where CL is present (*6*).

CL is a unique mitochondrial lipid that is essential for mitochondrial enzyme function (*7*). It interfaces mitochondrial electron transport chain complexes III and IV and interacts with many other mitochondrial proteins, including the ADT-ATP carrier, phosphate carrier, and CL synthase (*8*). CL also sequesters cytochrome *c* in the inner membrane (IM). CL is vulnerable to oxidative attack due to its unsaturated fatty acid side chains and its proximity to ROS-producing sites. Peroxidation of CL occurs when ROS are produced during apoptosis (*9*), leading to a decreased affinity for cytochrome *c* (*10*) and dissociation of cytochrome *c* from the membrane for release (*11*). When peroxidation of CL is prevented by overexpression of mitochondrial phospholipid hydroperoxide glutathione peroxidase, cytochrome *c* release and apoptosis are inhibited (*12*). It remains unclear how tBid interacts with CL. Bid contains eight α-helices in which two

[†] This study is supported by the Elsa U. Pardee Foundation, the Huntsman Cancer Foundation, and the Massey Cancer Center (R.M.L.) and in part by Grant MT-7654 from the Canadian Institutes of Health Research (R.M.E).

* To whom correspondence should be addressed. R.M.L.: Massey Cancer Center, Virginia Commonwealth University, Richmond, VA 23298; phone, (804) 628-2086; fax, (804) 828-8079; e-mail, rlee5@vcu.edu. R.M.E.: Department of Biochemistry and Biomedical Sciences, McMaster University, Hamilton, ON L8N 3Z5, Canada; phone, (905) 525-9140, ext. 22073; fax, (905) 521-1397; e-mail, epand@mcmaster.ca.

[‡] Department of Pharmaceutics and Pharmaceutical Chemistry, University of Utah.

[§] McMaster University.

[||] University of California, San Diego.

[⊥] Huntsman Cancer Institute, University of Utah.

[#] Virginia Commonwealth University.

[1] Abbreviations: PLS3, phospholipid scramblase 3; TNF-α, tumor necrosis factor α; CL, cardiolipin; ROS, reactive oxygen species; OM, outer membrane; IM, inner membrane; TUNEL, terminal deoxynucleotidyl transferase (TdT)-mediated dUTP nick end labeling; SEM, standard error of the mean.

10.1021/bi701962c CCC: $40.75
Published on Web 03/22/2008

central hydrophobic helices 6 and 7 are surrounded by other helices. NMR studies of the conformation of tBid revealed that there is no membrane insertion, and the helices of tBid are nearly parallel to the lipid bilayer with helix 6 tilted 20° from the membrane surface (*13, 14*). This finding suggests that CL should be present on the outer leaflet of the mitochondrial outer membrane (OM) to interact with tBid. However, CL is synthesized in the mitochondrial IM (*8*), raising the question of how CL moves to the mitochondrial surface. Evidence supports the possibility that CL translocates from the inner leaflet to the outer leaflet of IM during apoptosis (*15, 16*). Our previous study of the CL distribution by ^{32}P labeling of phospholipids showed an increased level of CL in the OM after UV irradiation and overexpression of phospholipid scramblase 3 (PLS3) (*17*).

Phospholipid scramblase (PLS) is a family of calcium-dependent enzymes responsible for bidirectional movement of phospholipids between two compartments (*18*). Four members of the PLS family have been identified (*19*). PLS1 is present in the plasma membrane and may be responsible for translocation of phospholipids between the inner and outer leaflets (*20*). PLS2 is reported to be in the nucleus (*21*), whereas PLS3 is in mitochondria (*17, 22*). PLS4 has not been characterized. PLS3 plays an important role in mitochondrial respiratory function, morphology, and apoptotic response. We have shown that overexpression of inactive mutant PLS3(F258V), which abolishes the conserved calcium binding motif (*23*), suppressed mitochondrial respiration and resulted in a unique mitochondrial morphology with densely packed cristae (*17*). PLS3 is also the mitochondrial target in protein kinase C (PKC)-δ-induced apoptosis (*22*). Phosphorylation of PLS3 at Thr21 by PKC-δ increases the activity of PLS3 (*24*). In this study, we report that PLS3 regulates tBid-induced apoptosis by increasing the level of CL on the surface of mitochondria and production of ROS. PLS3 is also subjected to regulation by tBid and Bcl-2 to modulate apoptotic responses in mitochondria.

MATERIALS AND METHODS

Construction of Cells with Inducible Expression of PLS3. The cDNAs of PLS3 and PLS3(F258V) were cloned into the pIND plasmid (Invitrogen Inc., Carlsbad, CA). HeLa cells were transfected with constructs of ecdysone-inducible pIND-PLS3 or pIND-PLS3(F258V) and pVgRXR, which encodes the ecdysone receptor. Cells were selected in 500 μg/mL G418 and 500 μg/mL Zeocin for 3 weeks, and single clones were isolated by limiting dilution. Clones were screened by incubation with ponasterone A (10 μM) for 48 h, and positive clones were identified by Western blotting with a PLS3 antibody. All experiments were performed with clones after induction for 48 h with ponasterone A.

Downregulation of PLS3 by siRNA. siRNA 283 and 309 were generated by Qiagen against nucleotides 283−304 and 309–330 of human PLS3, the sequences of which do not match other sequences in GenBank. A scrambled siRNA was synthesized as a negative control. HeLa cells were transfected with siRNA using Lipofectamine 2000 according to the manufacturer's protocol (Invitrogen Inc.) 1 day after seeding. Cells were harvested 48 h after transfection.

TUNEL Apoptosis Assay. Apoptosis was quantified by a TUNEL apoptosis assay [terminal deoxynucleotidyl transferase (TdT)-mediated dUTP nick end labeling]. Briefly, TNF-α-treated cells were fixed with 1% paraformaldehyde and incubated with TdT enzyme and FITC-labeled dUTP as described by the manufacturer's protocol (Roche Biotechnology). The percentages of apoptotic cells were quantified by flow cytometry.

Subcellular Fractionation and Cytochrome c Release Study. Mitochondria were isolated by differential centrifugation as described previously (*17, 22*). The cytoplasmic fractions were centrifuged again at 10000*g* to remove heavy membranes. Mitochondria and cytoplasmic fractions were analyzed by Western blotting using a cytochrome *c* antibody (BD Pharmingen, San Diego, CA). Bid antibody was generated by immunization of chicken with full-length Bid (Aves Laboratories, Inc., Tigard, OR).

NAO Staining. Cells (1×10^6) were incubated with the various concentrations of NAO for 15 min after fixation with 1% formaldehyde. The red fluorescence was measured by flow cytometry (*15*). The median fluorescence values were used to calculate the percentages using the red fluorescence of HeLa control cells incubated with 35 μM NAO as 100% saturation. This method was used by Garcia Fernandez et al. (*15, 16*) to quantify the percentages of CL in different mitochondrial membrane compartments.

Determination of the tBid Binding Capacity on the Mitochondrial Surface. Recombinant tBid(G94E) protein was produced as described previously (*25*). The protein was then labeled with FITC at a ratio of 1000:45 (micrograms) in a carbonate−bicarbonate buffer (pH 9) at 4 °C overnight. Excessive FITC was removed by a G25 gel filtration column (Amersham-Pharmacia Biotech, Piscataway, NJ). Purified FITC-tBid(G94E) was incubated with isolated mitochondria in a buffer [250 mM sucrose, 20 mM HEPES, 10 mM KCl, 3 mM KH_2PO_4, 1.5 mM $MgCl_2$, 1 mM EGTA, and 0.5 mg/mL BSA (pH 7.4)] at room temperature for 30 min. The mixtures were centrifuged at 10000*g* to separate mitochondria from supernatants. Mitochondria were washed five times with the isolation buffer, and fluorescence activities were measured by a microplate reader (Bio-Tech).

Preparation of PLS3-Containing Proteoliposomes. Recombinant PLS3 was produced by the bacterial expression system and purified by nickel affinity beads under denaturing conditions (6 M urea). Enzymatically active PLS3 was then obtained by refolding the denatured protein by steadily decreasing the urea concentrations followed by dialysis. The refolded PLS3 protein was then reconstituted into proteoliposomes. Briefly, a lipid mixture resembling the composition of the mitochondrial OM with 12% CL (*5*) in total lipids was dissolved in a chloroform/methanol mixture and dried as a film in the walls of a tube with nitrogen gas. The films were dissolved in a buffer containing sodium cholate (5%) and PLS3 protein via vortexing. Protein/lipid solutions, at specific lipid to protein ratios, were dialyzed against a buffer containing BioBeads SM2, 50–100 mesh (Bio-Rad). Dialyzed samples were transferred to silanized Eppendorf tubes, mixed with a very small amount of BioBeads SM2 for 20 min in an ice bath with frequent shaking, and then centrifuged for 1 min at 200*g*. The supernatant was transferred into clean silanized Eppendorf tubes for experiments. Liposomes were tested with BaxΔC, which is known to promote lipid flip-flop and serves as a positive control (*26*). The size of liposomes was determined by QUELS (quasi-elastic light

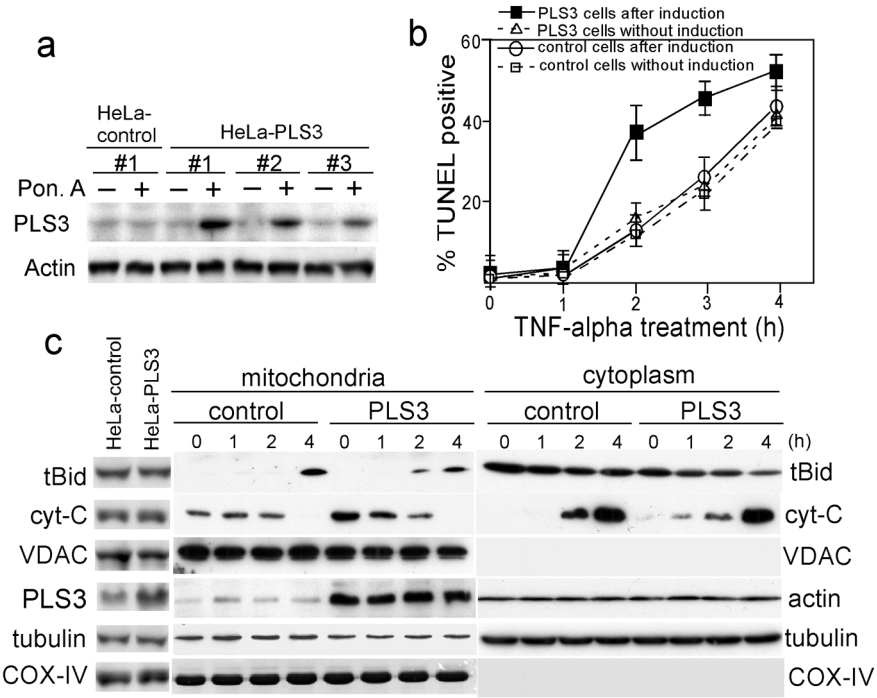

FIGURE 1: Upregulation of PLS3 enhances TNF-α-induced cytochrome *c* release and apoptosis. (a) Generation of inducible PLS3-expressing cells. HeLa cells were cotransfected with pVgRXR and pIND, pIND-PLS3, or pIND-PLS3(F258V) and selected with G418 and Zeocin. Clones were analyzed for PLS3 expression after induction with ponasterone A for 48 h. One randomly picked clone selected from cells transfected with pIND empty vector was used as a control (HeLa control). Clones 1, 2, and 3 were cells transfected with pIND-PLS3 (HeLa-PLS3). (b) PLS3 enhances TNF-α-induced apoptosis. Cells were induced with ponasterone A for 48 h and then treated with TNF-α (100 ng/mL) and cycloheximide (50 μM) to induce apoptosis. Cells were harvested at 0, 1, 2, 3, and 4 h for TUNEL assays. Error bars indicate SEM in four experiments. (c) Overexpression of PLS3 accelerates mitochondrial targeting of tBid and cytochrome *c* release. Cells were treated with TNF-α and cycloheximide followed by subcellular fractionation. The first two lanes are whole cell lysates from untreated HeLa control and HeLa PLS3 cells. Subsequent lanes are mitochondrial and cytoplasmic fractions from TNF-α-treated cells analyzed by Western blotting with antibodies against tBid, cytochrome *c*, and other marker proteins such as VADC, actin, tubulin, and cytochrome *c* oxidase (COX-IV) as the loading control.

scattering) as described previously (*26*) and was found to vary in different reconstitutions. Systems reported here correspond to an average size of 80 nm.

Lipid Flip-Flop Assay. Recombinant Bid was produced as a glutathione *S*-transferase fusion protein in BL21 bacterial cells and purified by glutathione Sepharose 4B affinity beads. tBid was produced by cleavage with full-length Bid with recombinant caspase 8 (Calbiochem) before usage. 1-Lauroyl-2-(1′-pyrenebutyroyl)-*sn*-glycero-3-phosphocholine (pyrene-10-PC) (Avanti Polar Lipids, Alabaster, AL) was used as a probe and incorporated into the outer monolayer of preformed PLS3-containing proteoliposomes so that the probe was 10% of the lipids in the outer monolayer or 5% of the total lipids. The rate of transbilayer diffusion of pyrene-10-PC was measured as previously described (*26, 27*). When flip-flop occurs, there is a reduction in the excimer emission because of dilution of the probe from one monolayer to two. The ratio of the excimer (I_e, emission at 476 nm) to monomer emission (I_m, emission at 397 nm) was measured as a function of time before and after the addition of ionomycin, 2 mM $CaCl_2$, and/or apoptotic proteins. The fluorescence experiments were carried out in 2 mL silanized glass cuvettes at 37 °C with PLS3 proteoliposomes at different lipid:protein ratios, and a lipid concentration of 25 μM. After addition of a freshly prepared solution of probe to the liposomes, the excimer:monomer emission ratio was monitored prior to addition of proteins or calcium until a plateau was reached. Measurements were taken with two independent preparations. Values of the I_e/I_m ratio were normalized to that of the proteoliposomes alone and then averaged. Excitation was 344 nm. The initial ratio at time zero was set to 1 to compare values for different conditions.

RESULTS

PLS3 Regulates TNF-α-Induced Apoptosis. To investigate the role of PLS3 in the regulation of tBid-induced apoptosis, we used TNF-α to activate caspase 8 and ultimately generate tBid, which translocates to mitochondria to induce cell death (*28, 29*). HeLa cells were stably transfected with ecdysone-inducible PLS3 (HeLa-PLS3), and expression was induced with ponasterone A [clones 1–3 (Figure 1a)]. Clone 1 was used for subsequent experiments for higher-level expression. HeLa control cells [clone 1 (Figure 1a)] were also generated with the pIND vector. Cells were incubated with TNF-α and cycloheximide, which was added to block the NF-κB pathway to activate the caspase 8/tBid pathway (*28*). More apoptosis was detected in HeLa-PLS3 cells compared to HeLa control cells 2 and 3 h after TNF-α treatment. At 4 h, the difference was less dramatic because both cells exhibited significant apoptosis (Figure 1b). Subcellular fractions revealed the appearance of tBid in mitochondria of HeLa-PLS3 cells 2 h after TNF-α treatment, but not in control cells (Figure 1c). The release of cytochrome *c* to the cytoplasm of HeLa-PLS3 cells appeared 1 h after TNF-α treatment, but no release was seen in similarly treated HeLa control cells (Figure 1c). The rates of cytochrome *c* release and tBid targeting to mitochondria increased at 4 h

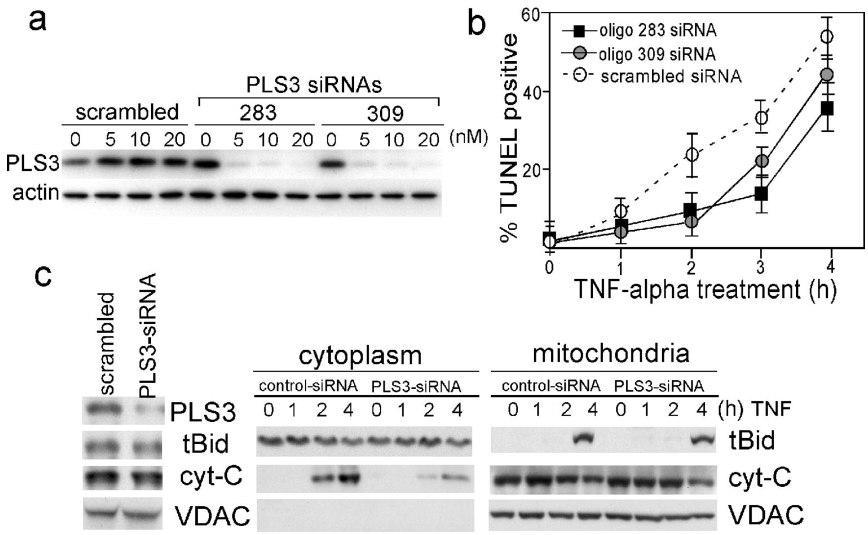

FIGURE 2: Downregulation of PLS3 suppresses TNF-α-induced apoptosis. (a) Downregulation of PLS3 by siRNAs. HeLa cells were transfected with scrambled control siRNA or PLS3 siRNA 283 or 309 at the indicated concentrations, and PLS3 levels were analyzed by Western blotting after 48 h. Actin was used as the loading control. (b) Downregulation of PLS3 suppresses TNF-α-induced apoptosis. HeLa cells transfected with PLS3 siRNA 283, 309, or scrambled control were incubated with TNF-α and cycloheximide. Cells were harvested at 0, 1, 2, 3, and 4 h for TUNEL assays. Error bars indicate SEM in three experiments. (c) Cytochrome *c* release in siRNA-transfected cells. HeLa cells were transfected with scrambled siRNA or PLS3 siRNAs 283 and incubated with TNF-α and cycloheximide. The first two lanes are whole cell lysates from cells processed simultaneously as in panel a to confirm the downregulation of PLS3. Mitochondria and cytoplasmic fractions from TNF-α-treated cells were probed with antibodies against tBid, cytochrome *c*, and VDAC by Western blotting.

when most of cells became apoptotic after TNF-α treatment. The time frame of these events was consistent with apoptosis detected by TUNEL assays (Figure 1b).

Next, we employed siRNA to downregulate PLS3. Two siRNA oligos 283 and 309 were capable of suppressing PLS3 expression compared with the scrambled siRNA control (Figure 2a). When HeLa cells were transfected with 283 or 309 siRNAs, TNF-α-induced cell death was suppressed compared with cells transfected with control siRNA (Figure 2b). Western blotting of the mitochondrial and cytoplasmic fractions revealed that cytochrome *c* released from mitochondria was suppressed when PLS3 was downregulated by 283 or 309 siRNAs (Figure 2c). Targeting of tBid to mitochondria and cytochrome *c* release did not change dramatically in cells transfected with PLS3 siRNAs (Figure 2c). Therefore, PLS3 is an important regulator of tBid-induced cytochrome *c* release from mitochondria.

Regulation of the Distribution of CL in the OM by PLS3. Next, we investigated the mechanism by which PLS3 enhances tBid-induced cytochrome *c* release. Because NMR studies show that tBid does not insert into the membrane (*13, 14*), modulation of the amount of CL on the mitochondrial surface by PLS3 may regulate tBid targeting. We utilized NAO to determine CL distribution in membrane bilayers, based on differential emission of NAO upon binding CL (*15, 16, 30*). When NAO binds CL at a 1:1 ratio, there is emission at 525 nm (green) and emission at 640 nm (red) when two molecules of NAO bind to one molecule of CL (*31, 32*). As CL becomes saturated with NAO in different leaflets of the membrane, the red fluorescence intensity not only correlates with the amount of CL but also provides information about its distribution. CL in the OM is saturated earlier than IM, and the outer leaflet of the membrane is saturated earlier than inner leaflet. Theoretically, there would be four plateaus, representing CL in the outer and inner leaflets of OM and IM, respectively. We optimized conditions for detecting CL in the OM by utilizing low concentrations of NAO to analyze the first two plateaus in cells with up- or downregulation of PLS3. All experiments were performed in formaldehyde-fixed cells to eliminate any possible influence by mitochondrial potential in NAO binding. Throughout the curves, the median fluorescence intensity was higher in HeLa-PLS3 and lower in HeLa-PLS3(F258V) cells compared to HeLa control cells (Figure 3a). Using the maximal fluorescence intensity of HeLa control cells as 100%, we calculated and plotted the percentage of CL at each concentration of NAO. A multiphasic pattern was observed in HeLa control and HeLa-PLS3 cells (Figure 3b,c), which was consistently reproducible in four experiments. The first two dips of plateaus (marked by 1 and 2 in Figure 3b,c), representing saturation of CL in outer and inner leaflets of OM, occurred at 4.25 and 5.0 μM NAO in control cells (Figure 3b) and 4.5 and 6.0 μM NAO in HeLa-PLS3 cells (Figure 3c). The corresponding percentages of CL were 8.20 and 9.69%, respectively, in the lowest points of dips 1 and 2 in control cells and increased to 9.95 and 14.56%, respectively, in those of HeLa-PLS3 cells. By contrast, the percentages of CL at the third dip at 10 μM NAO were 26.41% in control cells and decreased to 15.1% in HeLa-PLS3 cells (Figure 3e), suggesting that CL may be translocated from IM to OM upon overexpression of PLS3. In addition, the dips were more pronounced in HeLa-PLS3 cells, whereas the dips were flatter in HeLa cells expressing PLS3(F258V), an inactive PLS3 mutant, than those in HeLa control cells (Figure 3b−d). The percentages of the first two dips in HeLa-PLS3(F258V) cells were 5.60 and 6.50%, respectively, which were much lower than those of HeLa control cells, suggesting that there is much less CL in the OM (Figure 3e). These findings are consistent with the theory of enhanced translocation of CL to the OM by PLS3 and suppression of CL translocation by PLS3(F258V).

Similar studies were performed in HeLa cells transfected with PLS3 siRNA 283 or control siRNA (Figure 4a−d). Consistent with the results from HeLa-PLS3(F258V) cells,

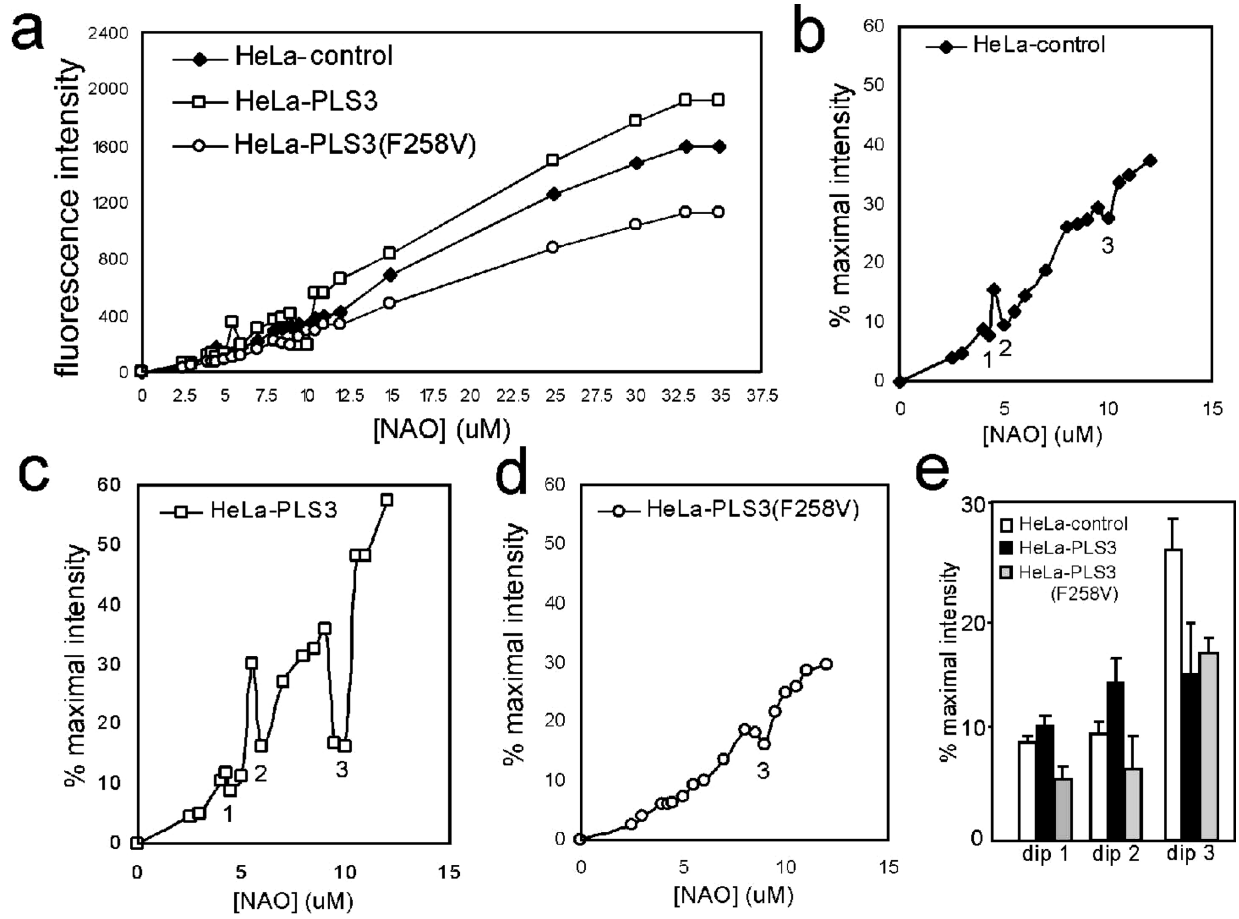

FIGURE 3: Determination of the distribution of CL by NAO. Cells were stained with different concentrations of NAO, and the median fluorescence intensity at 640 nm was determined by flow cytometry and plotted against the concentrations of NAO. (a) NAO fluorescence intensity in HeLa control, HeLa-PLS3, and HeLa-PLS3(F258V) cells. (b) Percentages of fluorescence intensity vs the maximal intensity in HeLa control cells. The median fluorescence intensity value of 35 μM NAO was considered to be 100% and used to calculate the percentage in each NAO concentration. Three dips were indicated by numbers, which correspond to the outer and inner leaflets of OM and IM, respectively. (c) Percentages of fluorescence intensity vs the maximal intensity in HeLa-PLS3 cells. The median fluorescence intensity value of 35 μM NAO in HeLa control cells was considered to be 100% and used to calculate the percentage in each NAO concentration from HeLa-PLS3. (d) Percentages of fluorescence intensity vs the maximal intensity in HeLa-PLS3(F258V) cells. A similar calculation was performed as described for panel c. The first two dips became less distinct. (e) Percentages of the lowest points of the three dips in HeLa control, HeLa-PLS3, and HeLa-PLS3(F258V) cells. Shown are the results of averages from three independent experiments.

the total amount of CL was reduced when PLS3 was downregulated by siRNA (Figure 4a). The first two plateaus in HeLa-siRNA 283 cells also became less distinct than those of the HeLa-siRNA control cells (Figure 4b−d), suggesting a decrease in the level of CL in the OM. These data support our theory that PLS3 regulates the level of CL on mitochondrial OM.

PLS3 Regulates tBid Binding Capacity on the Mitochondrial Surface We then developed a second assay to determine tBid binding capacity on the mitochondria surface using a fluorescently labeled probe that binds CL but does not insert into the membrane. tBid(G94E), a tBid mutant with an inactive BH3 domain, does not bind Bcl-2 or induce apoptosis (*28*) but has the same affinity for CL as wild-type tBid (*25*) and is targeted to mitochondrial CL in vivo (*33*). We conjugated the recombinant tBid(G94E) protein with FITC as a fluorescent probe for quantification of CL on the mitochondrial surface. After incubation with FITC-tBid(G94E), mitochondria from HeLa-PLS3 cells bind FITC-tBid(G94E) more than those from HeLa control cells, suggesting more CL on the surface after PLS3 overexpression. In contrast, mitochondria from HeLa-PLS3(F258V) cells retained less FITC activity than those from control cells (Figure 5a,b), suggesting less CL on the surface when mutant PLS3 is overexpressed. Similarly, studies of tBid binding capacity were also performed in HeLa cells transfected with siRNA 283. Cells transfected with PLS3 siRNA exhibited a decrease in the level of FITC-tBid(G94E) binding to mitochondria (Figure 5c,d). Therefore, PLS3 could regulate the distribution of CL on the mitochondrial surface.

PLS3 Regulates Mitochondrial Membrane Potential, Oxidative Phosphorylation, and ROS Production. Since PLS3 regulates the distribution of CL, we asked whether targeting PLS3 may also interfere with mitochondrial functions closely coupled to CL. Mitochondrial potential was first determined by fluorescent dye MitoTracker. No change was observed in HeLa control and HeLa-PLS3 cells (Figure 6a). However, production of ROS was assessed by staining cells with 2′,7′-dichlorodihydrofluorescein diacetate (H_2DCFDA) dye. Overexpression of PLS3 increased ROS production (Figure 6b), which was consistent with our previous report (*17, 22*). Next, we investigated the electron transport chain to determine the mechanism of the increased level of ROS. By sequential addition of substrates and inhibitors of electron transport

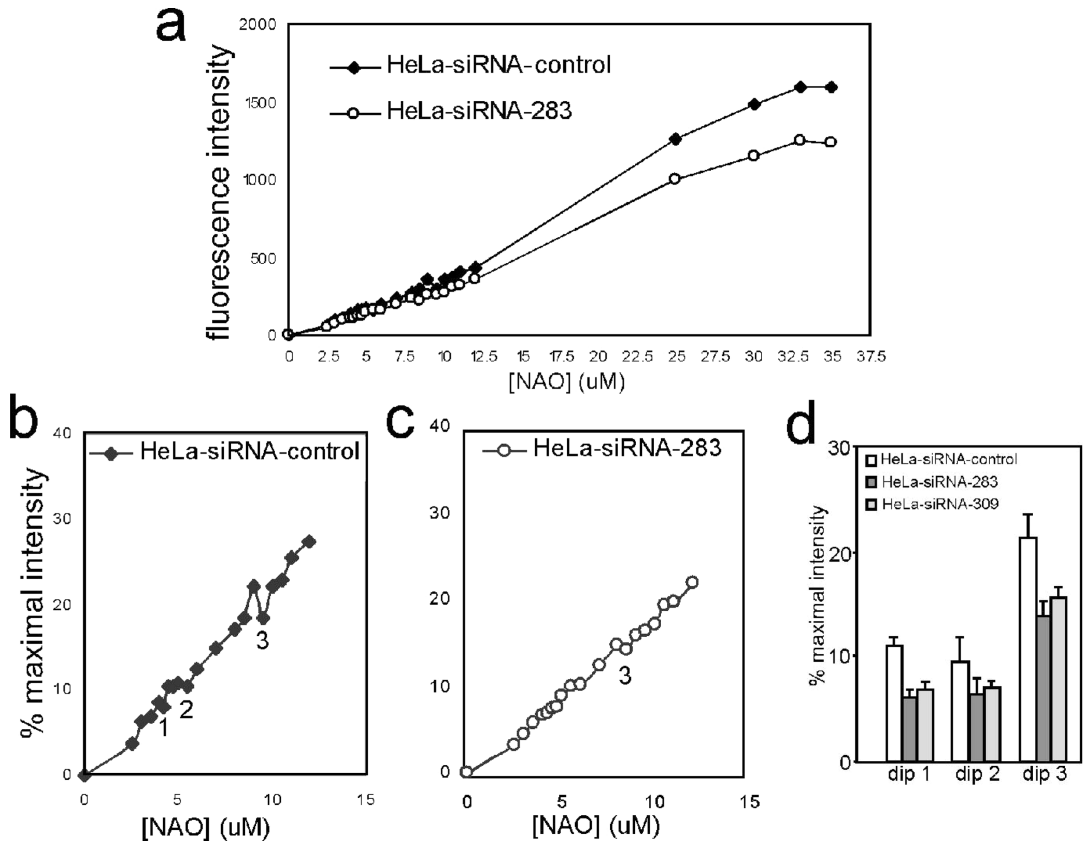

FIGURE 4: Effect of downregulation of PLS3 in CL distribution. Cells were transfected with PLS3 siRNA 283 or scrambled control siRNA and stained with different concentrations of NAO for flow cytometry as in Figure 3. The median fluorescence intensity was plotted vs NAO concentration as in Figure 3 to examine CL distribution. (a) Comparison of absolute fluorescence intensities in HeLa-siRNA control and HeLa-siRNA 283 cells. (b) Percentages of fluorescence intensity vs the maximal intensity in HeLa-siRNA control cells. The median fluorescence intensity value of 35 μM NAO in HeLa-siRNA control cells was considered to be 100% and used to calculate the percentage in each NAO concentration. The three dips are identified as described in the legend of Figure 2. (c) Percentages of fluorescence intensity vs maximal intensity in HeLa-siRNA 283 cells. Similar percentages are calculated as described for panel b, but the first two dips became less distinct. (d) Percentages of the lowest points of the three dips in HeLa-siRNA control, HeLa-siRNA 283, and HeLa-siRNA 309 cells. Shown are the results of averages from three independent experiments.

chain complexes, we first showed a normal oxygen consumption profile in control mitochondria (Figure 6c). Mitochondria from HeLa-PLS3 cells had normal oxygen consumption after addition of malate or succinate as substrates for Complex I and II, but oxygen consumption could not be blocked by either rotenone or antimycin (Figure 6d). Final addition of TMPD, a direct electron donor for Complex IV, induced the same rate of oxygen consumption as in control mitochondria (Figure 6d). These data suggest dysfunction in Complexes I and III in HeLa-PLS3 cells, and the function of Complex IV was not affected by PLS3. A similar pattern of rotenone resistance has been described in Complex I mutation (*34*). Thus, overexpression of PLS3 may cause mitochondrial changes in Complexes I and III, the most common sites for ROS production (*35, 36*). The enhanced ROS production in HeLa-PLS3 cells could contribute to peroxidation of CL and mobilization of cytochrome *c* (*10*) for release (*11*).

Development of a Transbilayer Lipid Flip-Flop Assay in PLS3 Proteoliposomes. Our preceding data suggest that PLS3 increases the amount of CL on the surface of mitochondria. Since PLS3 is a member of the scramblase family, PLS3 should have the capability of promoting transbilayer lipid diffusion, or lipid "flip-flop", like other members of the scramblase family. We prepared recombinant PLS3 (Figure 7a) and developed a lipid flip-flop assay to investigate the regulation of PLS3 (Figure 7b). The activity of PLS3 was tested in a lipid flip-flop assay using liposomes with a composition similar to that of the mitochondrial OM (*26*). Without addition of any cofactor, a small spontaneous rate of flip-flop was observed in PLS3-containing proteoliposomes, but similar baseline activity was also observed in liposomes without PLS3 (Figure 6c, before addition of Ca^{2+}). Calcium is known to be a cofactor for scramblase activity (*23*), but we detected little calcium-stimulated activity in PLS3 proteoliposomes (Figure 7c, after addition of Ca^{2+}). Pure phospholipid liposomes without PLS3 made by the same detergent dialysis procedure showed an artifactual increase in I_e/I_m (Figure 7c, top curve). This could occur if calcium increased the rate of lateral mobility of the pyrene-10-PC or as a consequence of increased light scattering caused by calcium-induced vesicle aggregation. Given the possibility that the calcium binding motif of PLS3 could be buried inside of liposomes and not accessible to calcium, we added ionomycin to increase the calcium concentration inside the proteoliposomes. Incubating the vesicles with PLS3 for 2 h with increasing concentrations of Ca^{2+} in the absence or presence of ionomycin, however, did not cause any increase in the level of lipid flip-flop with either the py-10-PC-based assay or an assay using a longer chain NBD-PE introduced into the liposomes during detergent dialysis (*37*) (data not shown).

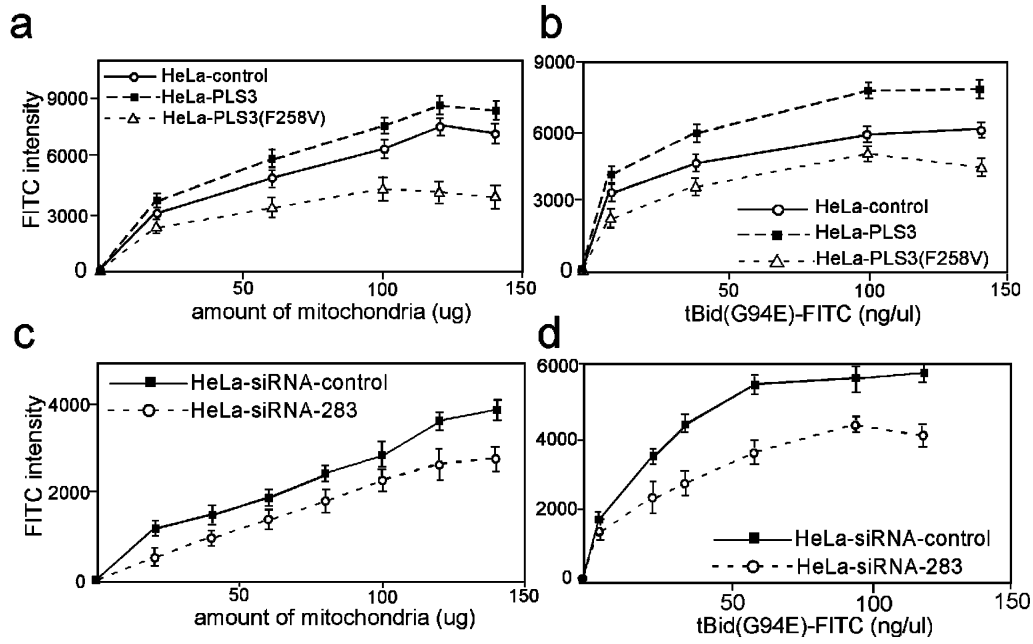

FIGURE 5: PLS3 regulates tBid binding capacity on the mitochondrial surface. (a) Mitochondria were isolated from HeLa control, HeLa-PLS3, and HeLa-PLS3(F258V) cells, then incubated with FITC-tBid(G94E) (20 ng) in 50 μL of binding buffer for 20 min, and washed five times with the binding buffer. The fluorescence activity of mitochondrial pellets was measured by a fluorescence microplate reader. Error bars indicate standard deviations of three independent experiments. (b) Mitochondria (50 μg by protein) from HeLa control, HeLa-PLS3, or HeLa-PLS3(F258V) cells were incubated with increasing amounts of FITC-tBid(G94E) in 50 μL of binding buffer for 20 min. Mitochondria were washed extensively, and fluorescence intensities of mitochondrial pellets were quantified. (c) Mitochondria from HeLa-siRNA 283 and HeLa-siRNA control cells were used for an experiment similar to that in panel a. (d) Mitochondria from HeLa-siRNA 283 and HeLa-siRNA control cells were used for the same experiment as in panel b.

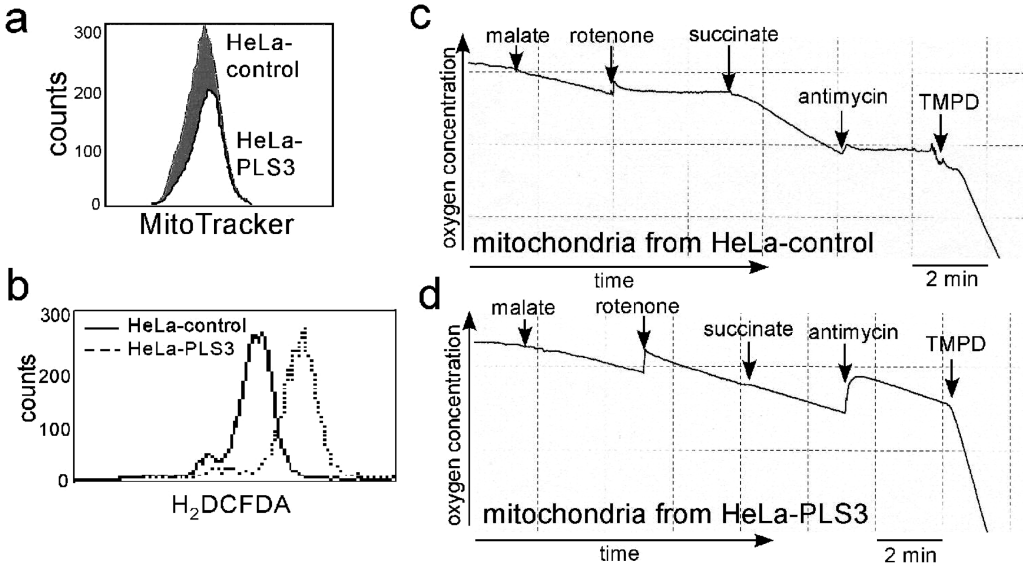

FIGURE 6: Effect of PLS3 on mitochondrial potential, ROS production, and oxidative phosphorylation. (a) Effect of PLS3 overexpression in mitochondrial potential. (b) Generation of ROS in HeLa-PLS3 cells. HeLa control and HeLa-PLS3 cells are incubated with 10 μM H_2DCFDA followed by flow cytometry analysis. (c and d) Comparison of oxygen consumption of mitochondria from HeLa control and HeLa-PLS3 cells. Isolated mitochondria (50 μg) were incubated in the chamber of the Mitocell, and the oxygen concentration was monitored continuously with the oxygen meter. Substrates and inhibitors of the electron transport chain complexes were added sequentially to determine the effect. Rotenone suppressed malate-induced oxygen consumption (Complex I). Antimycin suppressed succinate-induced respiration (Complex III). The effect of TMPD confirms the integrity of mitochondrial respiratory complexes. Each grid in the horizontal axis is a 2 min interval. The bottom panel shows the result of mitochondria isolated from HeLa-PLS3 cells. Both rotenone and antimycin failed to suppress the oxygen consumption.

PLS3 Activation Requires both Calcium and tBid. Previously, Bid as well as tBid alone has been reported to have lipid transferase activity (*38*). Given our finding that PLS3 enhances tBid-induced apoptosis, we incorporated tBid into the lipid flip-flop assay. In proteoliposomes containing PLS3, we observed that tBid activated the scramblase activity of PLS3 in a Ca^{2+}-dependent manner, while tBid alone, unlike Bax (*26*), added in the absence of Ca^{2+} had little effect on the flip-flop rate (Figure 7d). The flip-flop rate was more rapid (indicated by a decrease in the I_e/I_m ratio) in PLS3 proteoliposomes along with both tBid and Ca^{2+} than in pure lipid liposomes treated with tBid only (Figure 7d). Similar

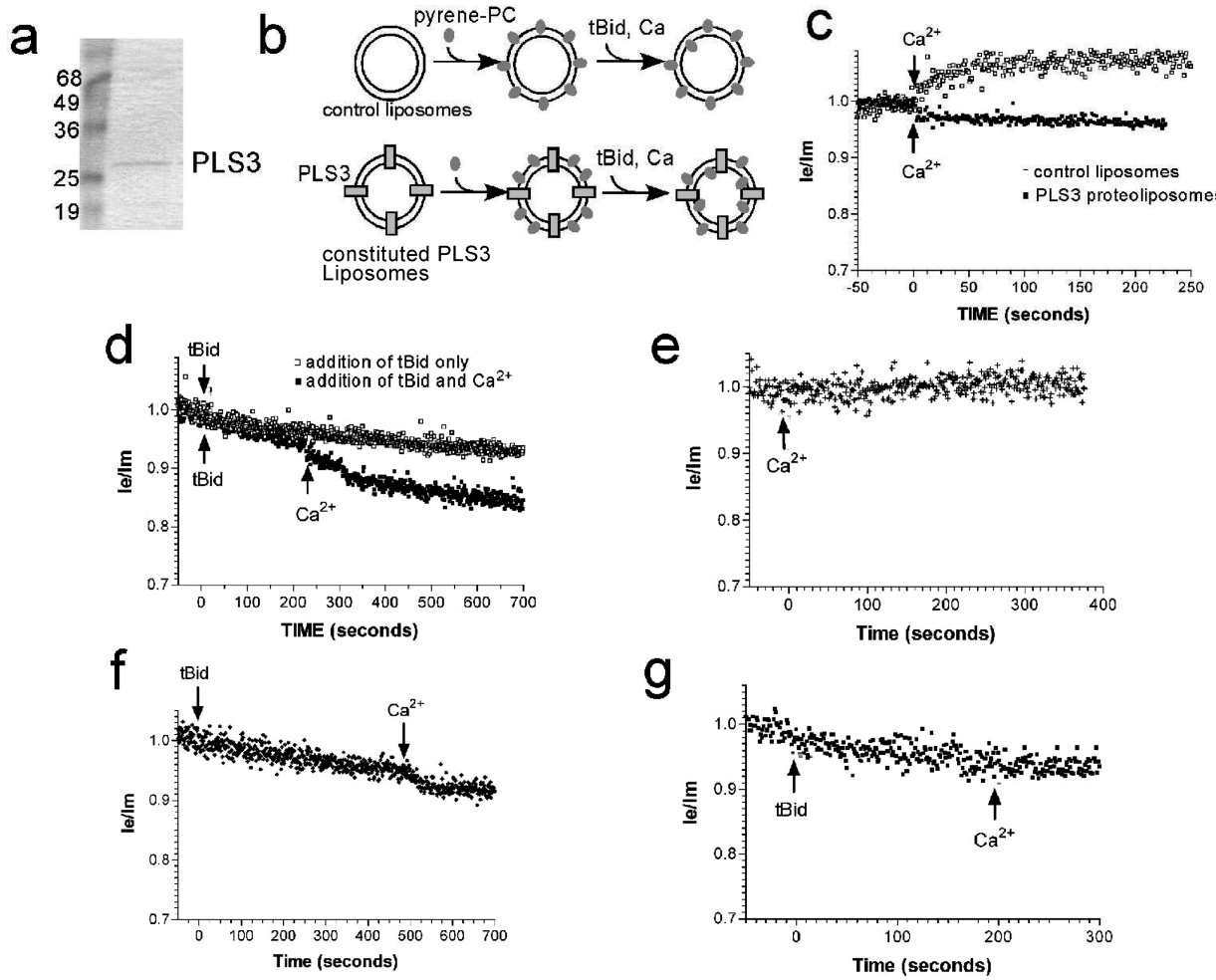

FIGURE 7: Regulation of PLS3 activity in the lipid flip-flop assay. (a) Coomassie staining of the purified PLS3. (b) Schematic diagram of the phospholipid flip-flop assay.The pyrene-PC (gray dots) was used as a probe to quantify the flip-flop, which is determined by the ratio of excimer and monomer (I_e/I_m). (c) Control liposomes have minimal lipid flip-flop. The top curve (□) shows data for reconstituted liposomes without PLS3 with 2 mM Ca^{2+} added at time zero. The bottom curve (■) shows data for reconstituted PLS3 proteoliposomes with 2 mM Ca^{2+} added at time zero. No lipid flip-flop activity was seen. (d) Activation of PLS3 requires tBid in the presence of Ca^{2+}. The top curve (□) shows data for reconstituted PLS3 proteoliposomes with 160 nM tBid added at time zero. The bottom curve (■) shows data for reconstituted PLS3 proteoliposomes with 160 nM tBid added at time zero and 2 mM Ca^{2+} added at 200 s. The lipid:protein ratio in these two curves is 300:1. (e and f) Transbilayer lipid diffusion in proteoliposomes reconstituted with mutant PLS3(F258V). Mutant PLS3(F258V) or wild-type PLS3 (WT) was reconstituted into liposomes at a final lipid:protein ratio of 100:1. (e) Ca^{2+} (2 mM) was added at time zero. (f) tBid (160 nM) at time zero and 2 mM Ca^{2+} at 500 s were added. (g) Mutant and WT PLS3 reconstituted together in an equimolar mixture. tBid (160 nM) was added at time zero and Ca^{2+} at 200 s.

results in the presence of tBid and calcium were obtained over a range of lipid:PLS3 protein ratios (not shown), showing that the effect is reproducible. This PLS3 assay was confirmed using a different method described by McIntyre and Sleight (*37*) (results not shown).

The PLS3(F258V) mutant, which has a mutation in the Ca binding motif, showed no flip-flop activity in the presence of calcium (Figure 7e) and only slight activity upon addition of both tBid and Ca^{2+} (Figure 7f). Furthermore, when wild-type PLS3 was reconstituted into liposomes together with the PLS3(F258V) mutant, the flip-flop activity of wild-type PLS3 was completely inhibited even in the presence of tBid and Ca^{2+} (Figure 7g), suggesting that PLS3(F258V) could serve as a dominant negative mutant of PLS3. This finding explains the previous result that expression of the PLS3(F258V) mutant in 293 cells can still exhibit a phenotype consistent with low PLS3 activity despite the presence of normal PLS3 in these cells (*26*). Finally, the spontaneous rate of flip-flop seen with the scramblase is eliminated in the mutant (Figure 7e), suggesting that there is a stabilizing effect of the PLS3(F258V) mutant on the proteoliposomes. These results provide strong support that tBid acts by activating the wild-type PLS3 protein in a calcium-dependent manner. Furthermore, the loss of flip-flop activity with this mutation shows that stimulation of this process has some degree of specificity and that this process is not stimulated by just any integral membrane protein. Taken together, these studies validate a calcium-dependent lipid trafficking machinery involving tBid and PLS3 subsequent to targeting of tBid to mitochondria.

Bcl-2 Prevents tBid-Induced PLS3 Activation. Because Bcl-2 inhibits the apoptotic effect of tBid (*28*), we investigated whether Bcl-2 prevented tBid-induced PLS3 activation in the lipid flip-flop assay. Bcl-2 was first incubated with tBid at an equimolar ratio for 5 min and then added to proteoliposomes reconstituted with PLS3 at time zero. After incubation for several minutes, calcium was added. No lipid flip-flop activity was observed in the presence of Bcl-2 (Figure 8a), indicating that Bcl-2 completely suppresses tBid-induced PLS3 activation. To explore this finding further, we tested whether the level of Bcl-2 was modulated in HeLa

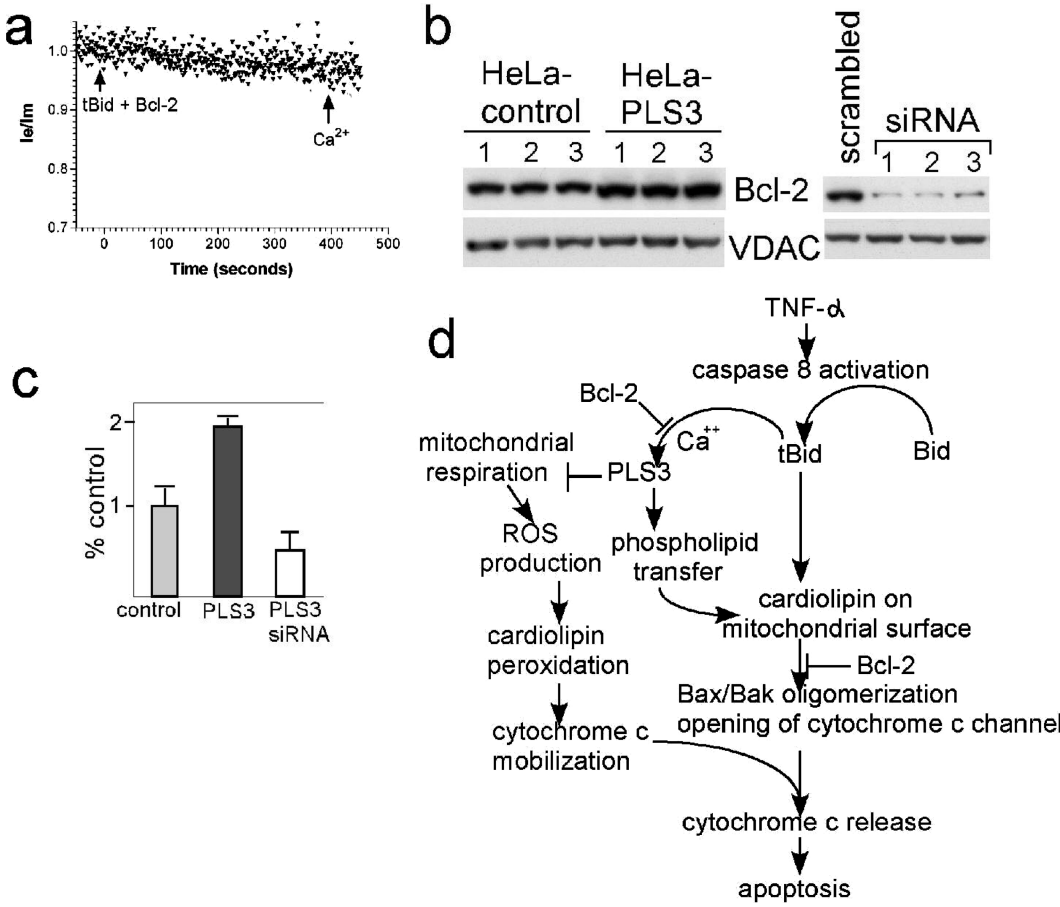

FIGURE 8: Effect of Bcl-2 on PLS3. (a) Bcl-2 suppresses tBid-induced PLS3 activation. PLS3 proteoliposomes were reconstituted at a lipid:protein ratio of 500. An equimolar mixture of 160 nM tBid and Bcl-2 protein was incubated for 15 min at room temperature before proteoliposomes were added at time zero; 2 mM Ca^{2+} was added at 400 s. The relationship among PLS3, tBid, cardiolipin, cytochrome *c* mobilization, and Bcl-2 is shown. See the Discussion for a detailed explanation. (b) Compensatory change in the Bcl-2 level in cells with up- or downregulation of PLS3. HeLa cells were transfected with PLS3 expression vector or empty vector. Three independent clones were selected for Western blotting with the Bcl-2 antibody. The right panel shows that HeLa cells were transfected with scrambled siRNA and PLS3-siRNA 283 in triplicate. Cell lysates were tested via Western blotting for the levels of Bcl-2. VDAC was used as a loading control for mitochondria. (c) Quantification of the data in panel b. The intensity of Bcl-2 bands was quantified and averaged. (d) Model of the effect of PLS3 on mitochondria in TNF-α-induced apoptosis. See the Discussion for details.

cells with overexpression or downregulation of PLS3. We found that the level of Bcl-2 was increased in mitochondria of HeLa-PLS3 cells compared with those of HeLa control cells (Figure 8b,c). In contrast, levels of Bcl-2 were diminished in mitochondria of HeLa cells transfected with siRNA 283 (Figure 8b,c), further supporting a regulatory role of Bcl-2 in PLS3.

DISCUSSION

The significance of CL in apoptosis has drawn much attention since it was discovered as the lipid receptor for tBid in mitochondria (*4*). Changes of CL in mitochondria after TNF-related apoptosis inducing ligand (TRAIL) treatment have been investigated by LC−MS (*39*), but that study evaluated only the overall amount of CL without considering the distribution of CL in mitochondria (*39*). CL in mitochondria is not distributed in a homogeneous pattern, and the contact site of IM and OM where CL clusters and segregates through creatine kinase (*40*) is the place where CL contributes to tBid targeting and regulation of cell death. If we examine the contact site even more closely, only CL present on the outer surface of OM will be able to interact with tBid given that membrane-associated tBid is in a conformation with its helices parallel to the surface without membrane insertion (*13, 14*). Hence, targeting of tBid could be regulated by the accessibility of CL on the surface of mitochondria. How does CL reach the outer surface of mitochondria since biosynthesis of CL is in the IM (*41*)? The answer to this question is suggested by a variety of changes in lipid metabolism, traffic, and remodeling during apoptosis (*38, 42–44*). Translocation of phosphatidylserine (PS) from the inner leaflet to the outer leaflet of the plasma membrane is a signal for phagocytosis of apoptotic cells (*45, 46*). However, due to the two-bilayer membrane structure in mitochondria, the CL trafficking machinery in mitochondria is likely to be more complicated than that in the plasma membrane. Lipid movement can occur within the IM or OM, between IM and OM, and between mitochondria and other organelles. Translocation of CL to the surface of the plasma membrane has been reported, which was used to explain the production of the anti-CL antibody in patients with anti-phospholipid syndrome (*47*). Lipid translocation between the mitochondrial IM and OM has not been studied because of various technical problems. Previously, we demonstrated that mitochondrial PLS3 could be the candidate enzyme responsible for moving CL from the IM to OM (*17*).

Here we investigate the effect of PLS3 in the regulation of CL on the mitochondrial surface by two approaches. The first is to use NAO for a semiquantification of CL distribution, but this methodology is difficult to interpret and the difference not dramatic. We then developed a FITC-tBid(G94E) probe to quantify the tBid binding capacity on the mitochondrial surface. Using this probe, it was confirmed that that PLS3 can indeed modulate the tBid binding capacity on the mitochondrial surface. We believe that the key issue for tBid targeting is not the total amount of CL in mitochondria, but rather the distribution of CL in the microenvironment of the outer surface of the mitochondrial contact site, where tBid can gain access since tBid does not penetrate the mitochondrial OM (*13, 14*). PLS3 is thus a critical member of the lipid trafficking machinery and could regulate TNF-α- or tBid-induced apoptosis. It is also worth noting that the tBid binding capacity quantified by the FITC-tBid(G94E) probe includes not only CL but also monolysocardiolipin (MLCL), a metabolite of CL that also binds tBid (*48*). Bcl-2 is unlikely responsible for changes of the tBid binding capacity because the FITC-tBid(G94E) probe has a defective BH3 domain and does not bind Bcl-2 (*28*).

The other effect of PLS3 overexpression is an increase in the level of de novo synthesis of CL and a decrease in the degree of CL remodeling (*49*). The combined effect of all these changes of CL compromises the function of oxidative phosphorylation, leading to generation of ROS. CL could therefore be in a more peroxidized status due to a high content of unsaturated fatty acid (*9, 36*). Its affinity for cytochrome *c* will be reduced (*10*). As indicated by Ott et al. (*11*), cytochrome *c* release is a two-step process and requires mobilization of cytochrome *c* from a membrane-bound status before it could be released during apoptosis. The increase in the amount of ROS in PLS3 overexpressers will provide the second mechanism by which cells with overexpression of PLS3 are prone to release cytochrome *c* even though there is a corresponding increase in Bcl-2 that controls the gate of cytochrome *c* release.

To study the regulation of PLS3 activity, we developed a lipid flip-flop assay based on the transbilayer movement of a pyrene-PC probe. The application of the lipid flip-flop assay in examining PLS3 activity allows us to demonstrate that tBid activates PLS3 in a calcium-dependent manner. This in vitro assay provided valuable information regarding the essential cofactors required for PLS3 activity. We are still in the process of developing a methodology for determining PLS3 activity in vivo to investigate any change in PLS3 activity after cells are treated with TNF-α. The lipid flip-flop assay of PLS3 also unveiled a novel function of Bcl-2 in blocking PLS3. Bcl-2 is known to block apoptosis induced by tBid, which was thought to be mediated by preventing Bax oligomerization and activation (*50*). Here we show that Bcl-2 inhibits tBid-induced PLS3 activation, which provides a second function for Bcl-2 in regulating tBid-induced Bax activation. Cells with up- or downregulation of PLS3 have a corresponding compensatory change in their Bcl-2 level, suggesting that the activity of PLS3 may need to be tightly regulated. We propose a model for regulation of TNF-α- and tBid-induced cytochrome *c* release as depicted in Figure 8d. When caspase 8 is activated after TNF-α treatment and Bid is cleaved to tBid, tBid targeting mitochondria requires the presence of CL on the mitochondrial surface. This process is regulated by the basal activity of PLS3. Without the lipid scrambling activity of PLS3, translocation of CL to the surface of mitochondria and tBid targeting will be compromised. Once tBid is targeted to mitochondria, it activates PLS3 to promote transport of CL to the outer surface of mitochondria and further enhances tBid targeting. A positive feedback loop thus forms and amplifies the apoptotic response. Negative control of this positive feedback loop is provided by Bcl-2, which blocks not only tBid-induced Bax activation but also the amplification loop between PLS3 and tBid.

What could be the positive regulator of this feedback loop? Previously, we found that PLS3 is the mitochondrial target of PKC-δ-induced apoptosis (*22*). PLS3 is phosphorylated by PKC-δ at threonine 21 (*51*), and phosphorylation increases the lipid flip-flop activity of PLS3 (*24*). Cell death enhancers such as AD198 (*51*) and PEP005 (*52*) induce PKC-δ and PLS3 activation to enhance tBid targeting and induction of cytochrome *c* release to cause cell death. Cell death induced by either UV irradiation or TRAIL treatment is also associated with a significant elevation of the level of mitochondrial diacylglycerol (DAG) (*39, 53*), a critical activator of PKC-δ. Activation of PKC-δ subsequently facilitates caspase 8 cleavage and enhances cell death (*39*). At the same time, activated PKC-δ in mitochondria could also induce PLS3 phosphorylation and activation to trigger CL changes in mitochondria and further enhance the process of cell death.

In conclusion, PLS3 is a mitochondrial enzyme that regulates translocation of lipid between mitochondrial inner and outer membranes. By enhancing translocation of CL to the mitochondrial surface, PLS3 enhances targeting of tBid to mitochondria. Subsequently, tBid further activates PLS3 and forms a positive feedback loop. Bcl-2 serves as a negative regulator, and PKC-δ serves as the positive regulator of this positive feedback loop formed by PLS3, CL, and tBid.

ACKNOWLEDGMENT

We are grateful to Dr. Jean-Claude Martinou for providing us with samples of tBid with which some of the initial flip-flop studies were conducted.

REFERENCES

1. Li, P., Nijhawan, D., Budihardjo, I., Srinivasula, S. M., Ahmad, M., Alnemri, E. S., and Wang, X. (1997) Cytochrome c and dATP-dependent formation of Apaf-1/caspase-9 complex initiates an apoptotic protease cascade. *Cell 91*, 479–489.
2. Wei, M. C., Lindsten, T., Mootha, V. K., Weiler, S., Gross, A., Ashiya, M., Thompson, C. B., and Korsmeyer, S. J. (2000) tBID, a membrane-targeted death ligand, oligomerizes BAK to release cytochrome c. *Genes Dev. 14*, 2060–2071.
3. Yin, X. M., Wang, K., Gross, A., Zhao, Y., Zinkel, S., Klocke, B., Roth, K. A., and Korsmeyer, S. J. (1999) Bid-deficient mice are resistant to Fas-induced hepatocellular apoptosis. *Nature 400*, 886–891.
4. Lutter, M., Fang, M., Luo, X., Nishijima, M., Xie, X., and Wang, X. (2000) Cardiolipin provides specificity for targeting of tBid to mitochondria. *Nat. Cell Biol. 2*, 754–761.
5. Kuwana, T., Mackey, M. R., Perkins, G., Ellisman, M. H., Latterich, M., Schneiter, R., Green, D. R., and Newmeyer, D. D. (2002) Bid, bax, and lipids cooperate to form supramolecular openings in the outer mitochondrial membrane. *Cell 111*, 331–342.
6. Kim, T. H., Zhao, Y., Ding, W. X., Shin, J. N., He, X., Seo, Y. W., Chen, J., Rabinowich, H., Amoscato, A. A., and Yin, X. M. (2004) Bid-cardiolipin interaction at mitochondrial contact site contributes

to mitochondrial cristae reorganization and cytochrome c release. *Mol. Biol. Cell 15*, 3061–3072.
7. Hatch, G. M. (1998) Cardiolipin: Biosynthesis, remodeling and trafficking in the heart and mammalian cells. *Int. J. Mol. Med. 1*, 33–41.
8. Schlame, M., Rua, D., and Greenberg, M. L. (2000) The biosynthesis and functional role of cardiolipin. *Prog. Lipid Res. 39*, 257–288.
9. Petrosillo, G., Ruggiero, F. M., and Paradies, G. (2003) Role of reactive oxygen species and cardiolipin in the release of cytochrome c from mitochondria. *FASEB J. 17*, 2202–2208.
10. Shidoji, Y., Hayashi, K., Komura, S., Ohishi, N., and Yagi, K. (1999) Loss of molecular interaction between cytochrome c and cardiolipin due to lipid peroxidation. *Biochem. Biophys. Res. Commun. 264*, 343–347.
11. Ott, M., Robertson, J. D., Gogvadze, V., Zhivotovsky, B., and Orrenius, S. (2002) Cytochrome c release from mitochondria proceeds by a two-step process. *Proc. Natl. Acad. Sci. U.S.A. 99*, 1259–1263.
12. Nomura, K., Imai, H., Koumura, T., Kobayashi, T., and Nakagawa, Y. (2000) Mitochondrial phospholipid hydroperoxide glutathione peroxidase inhibits the release of cytochrome c from mitochondria by suppressing the peroxidation of cardiolipin in hypoglycaemia-induced apoptosis. *Biochem. J. 351*, 183–193.
13. Gong, X. M., Choi, J., Franzin, C. M., Zhai, D., Reed, J. C., and Marassi, F. M. (2004) Conformation of membrane-associated proapoptotic tBid. *J. Biol. Chem. 279*, 28954–28960.
14. Oh, K. J., Barbuto, S., Meyer, N., Kim, R. S., Collier, R. J., and Korsmeyer, S. J. (2005) Conformational changes in BID, a pro-apoptotic BCL-2 family member, upon membrane binding. A site-directed spin labeling study. *J. Biol. Chem. 280*, 753–767.
15. Garcia Fernandez, M., Troiano, L., Moretti, L., Pedrazzi, J., Salvioli, S., Castilla-Cortazar, I., and Cossarizza, A. (2000) Changes in intramitochondrial cardiolipin distribution in apoptosis-resistant HCW-2 cells, derived from the human promyelocytic leukemia HL-60. *FEBS Lett. 478*, 290–294.
16. Garcia Fernandez, M., Troiano, L., Moretti, L., Nasi, M., Pinti, M., Salvioli, S., Dobrucki, J., and Cossarizza, A. (2002) Early changes in intramitochondrial cardiolipin distribution during apoptosis. *Cell Growth Differ. 13*, 449–455.
17. Liu, J., Dai, Q., Chen, J., Durrant, D., Freeman, A., Liu, T., Grossman, D., and Lee, R. M. (2003) Phospholipid scramblase 3 controls mitochondrial structure, function, and apoptotic response. *Mol. Cancer Res. 1*, 892–902.
18. Bevers, E. M., Comfurius, P., Dekkers, D. W., and Zwaal, R. F. (1999) Lipid translocation across the plasma membrane of mammalian cells. *Biochim. Biophys. Acta 1439*, 317–330.
19. Wiedmer, T., Zhou, Q., Kwoh, D. Y., and Sims, P. J. (2000) Identification of three new members of the phospholipid scramblase gene family. *Biochim. Biophys. Acta 1467*, 244–253.
20. Zhou, Q., Zhao, J., Stout, J. G., Luhm, R. A., Wiedmer, T., and Sims, P. J. (1997) Molecular cloning of human plasma membrane phospholipid scramblase. A protein mediating transbilayer movement of plasma membrane phospholipids. *J. Biol. Chem. 272*, 18240–18244.
21. Yu, A., McMaster, C. R., Byers, D. M., Ridgway, N. D., and Cook, H. W. (2003) Stimulation of phosphatidylserine biosynthesis and facilitation of UV-induced apoptosis in Chinese hamster ovary cells overexpressing phospholipid scramblase 1. *J. Biol. Chem. 278*, 9706–9714.
22. Liu, J., Chen, J., Dai, Q., and Lee, R. M. (2003) Phospholipid Scramblase 3 Is the Mitochondrial Target of Protein Kinase Cδ-induced Apoptosis. *Cancer Res. 63*, 1153–1156.
23. Zhou, Q., Sims, P. J., and Wiedmer, T. (1998) Identity of a conserved motif in phospholipid scramblase that is required for Ca^{2+}-accelerated transbilayer movement of membrane phospholipids. *Biochemistry 37*, 2356–2360.
24. He, Y., Liu, J., Grossman, D., Durrant, D., Sweatman, T., Lothstein, L., Epand, R. F., Epand, R. M., and Lee, R. M. (2007) Phosphorylation of mitochondrial phospholipid scramblase 3 by protein kinase C-δ induces its activation and facilitates mitochondrial targeting of tBid. *J. Cell. Biochem. 101*, 1210–1221.
25. Liu, J., Weiss, A., Durrant, D., Chi, N. W., and Lee, R. M. (2004) The cardiolipin-binding domain of Bid affects mitochondrial respiration and enhances cytochrome c release. *Apoptosis 9*, 533–541.
26. Epand, R. F., Martinou, J. C., Montessuit, S., and Epand, R. M. (2003) Transbilayer lipid diffusion promoted by bax: Implications for apoptosis. *Biochemistry 42*, 14576–14582.
27. Muller, P., Schiller, S., Wieprecht, T., Dathe, M., and Herrmann, A. (2000) Continuous measurement of rapid transbilayer movement of a pyrene-labeled phospholipid analogue. *Chem. Phys. Lipids 106*, 89–99.
28. Luo, X., Budihardjo, I., Zou, H., Slaughter, C., and Wang, X. (1998) Bid, a Bcl2 interacting protein, mediates cytochrome c release from mitochondria in response to activation of cell surface death receptors. *Cell 94*, 481–490.
29. Li, H., Zhu, H., Xu, C. J., and Yuan, J. (1998) Cleavage of BID by caspase 8 mediates the mitochondrial damage in the Fas pathway of apoptosis. *Cell 94*, 491–501.
30. Gallet, P. F., Maftah, A., Petit, J. M., Denis-Gay, M., and Julien, R. (1995) Direct cardiolipin assay in yeast using the red fluorescence emission of 10-N-nonyl acridine orange. *Eur. J. Biochem. 228*, 113–119.
31. Petit, J. M., Huet, O., Gallet, P. F., Maftah, A., Ratinaud, M. H., and Julien, R. (1994) Direct analysis and significance of cardiolipin transverse distribution in mitochondrial inner membranes. *Eur. J. Biochem. 220*, 871–879.
32. Petit, J. M., Maftah, A., Ratinaud, M. H., and Julien, R. (1992) 10N-nonyl acridine orange interacts with cardiolipin and allows the quantification of this phospholipid in isolated mitochondria. *Eur. J. Biochem. 209*, 267–273.
33. Lutter, M., Perkins, G. A., and Wang, X. (2001) The pro-apoptotic Bcl-2 family member tBid localizes to mitochondrial contact sites. *BMC Cell Biol. 2*, 22.
34. Sabar, M., De Paepe, R., and de Kouchkovsky, Y. (2000) Complex I impairment, respiratory compensations, and photosynthetic decrease in nuclear and mitochondrial male sterile mutants of *Nicotiana sylvestris*. *Plant Physiol. 124*, 1239–1250.
35. Pitkanen, S., and Robinson, B. H. (1996) Mitochondrial complex I deficiency leads to increased production of superoxide radicals and induction of superoxide dismutase. *J. Clin. Invest. 98*, 345–351.
36. Turrens, J. F. (2003) Mitochondrial formation of reactive oxygen species. *J. Physiol. 552*, 335–344.
37. McIntyre, J. C., and Sleight, R. G. (1991) Fluorescence assay for phospholipid membrane asymmetry. *Biochemistry 30*, 11819–11827.
38. Esposti, M. D., Erler, J. T., Hickman, J. A., and Dive, C. (2001) Bid, a widely expressed proapoptotic protein of the Bcl-2 family, displays lipid transfer activity. *Mol. Cell. Biol. 21*, 7268–7276.
39. Sandra, F., Degli Esposti, M., Ndebele, K., Gona, P., Knight, D., Rosenquist, M., and Khosravi-Far, R. (2005) Tumor necrosis factor-related apoptosis-inducing ligand alters mitochondrial membrane lipids. *Cancer Res. 65*, 8286–8297.
40. Epand, R. F., Tokarska-Schlattner, M., Schlattner, U., Wallimann, T., and Epand, R. M. (2007) Cardiolipin clusters and membrane domain formation induced by mitochondrial proteins. *J. Mol. Biol. 365*, 968–980.
41. Ardail, D., Privat, J. P., Egret-Charlier, M., Levrat, C., Lerme, F., and Louisot, P. (1990) Mitochondrial contact sites. Lipid composition and dynamics. *J. Biol. Chem. 265*, 18797–18802.
42. Cristea, I. M., and Degli Esposti, M. (2004) Membrane lipids and cell death: An overview. *Chem. Phys. Lipids 129*, 133–160.
43. Esposti, M. D. (2002) Lipids, cardiolipin and apoptosis: A greasy licence to kill. *Cell Death Differ. 9*, 234–236.
44. Sorice, M., Circella, A., Cristea, I. M., Garofalo, T., Di Renzo, L., Alessandri, C., Valesini, G., and Esposti, M. D. (2004) Cardiolipin and its metabolites move from mitochondria to other cellular membranes during death receptor-mediated apoptosis. *Cell Death Differ. 11*, 1133–1145.
45. Fadok, V. A., Voelker, D. R., Campbell, P. A., Cohen, J. J., Bratton, D. L., and Henson, P. M. (1992) Exposure of phosphatidylserine on the surface of apoptotic lymphocytes triggers specific recognition and removal by macrophages. *J. Immunol. 148*, 2207–2216.
46. Fadok, V. A., and Henson, P. M. (2003) Apoptosis: Giving phosphatidylserine recognition an assist−with a twist. *Curr. Biol. 13*, R655–R657.
47. Sorice, M., Circella, A., Misasi, R., Pittoni, V., Garofalo, T., Cirelli, A., Pavan, A., Pontieri, G. M., and Valesini, G. (2000) Cardiolipin on the surface of apoptotic cells as a possible trigger for antiphospholipids antibodies. *Clin. Exp. Immunol. 122*, 277–284.
48. Esposti, M. D., Cristea, I. M., Gaskell, S. J., Nakao, Y., and Dive, C. (2003) Proapoptotic Bid binds to monolysocardiolipin, a new molecular connection between mitochondrial membranes and cell death. *Cell Death Differ. 10*, 1300–1309.
49. Van, Q., Liu, J., Lu, B., Feingold, K. R., Shi, Y., Lee, R. M., and Hatch, G. M. (2007) Phospholipid scramblase-3 regulates cardio-

lipin de novo biosynthesis and its resynthesis in growing HeLa cells. *Biochem. J. 401*, 103–109.
50. Cheng, E. H., Wei, M. C., Weiler, S., Flavell, R. A., Mak, T. W., Lindsten, T., and Korsmeyer, S. J. (2001) BCL-2, BCL-X(L) sequester BH3 domain-only molecules preventing BAX- and BAK-mediated mitochondrial apoptosis. *Mol. Cell 8*, 705–711.
51. He, Y., Liu, J., Durrant, D., Yang, H. S., Sweatman, T., Lothstein, L., and Lee, R. M. (2005) N-benzyladriamycin-14-valerate (AD198) induces apoptosis through protein kinase C-δ-induced phosphorylation of phospholipid scramblase 3. *Cancer Res. 65*, 10016–10023.
52. Hampson, P., Chahal, H., Khanim, F., Hayden, R., Mulder, A., Assi, L. K., Bunce, C. M., and Lord, J. M. (2005) PEP005, a selective small-molecule activator of protein kinase C, has potent antileukemic activity mediated via the δ isoform of PKC. *Blood 106*, 1362–1368.
53. Dai, Q., Liu, J., Chen, J., Durrant, D., McIntyre, T. M., and Lee, R. M. (2004) Mitochondrial ceramide increases in UV-irradiated HeLa cells and is mainly derived from hydrolysis of sphingomyelin. *Oncogene 23*, 3650–3658.

BI701962C